Supplementary Information:

Single molecule magnetoresistance with combined antiferromagnetic and ferromagnetic electrodes

Alexei Bagrets,[*,†,‡] Stefan Schmaus,[¶,§,@] Ali Jaafar,[‖] Detlef Kramczynski,[¶] Toyo Kazu Yamada,[¶,⊥] Mébarek Alouani,[‖] Wulf Wulfhekel,[¶,§] and Ferdinand Evers[‡,#]

Steinbuch Centre for Computing, Karlsruhe Institute of Technology, 76344 Eggenstein-Leopoldshafen, Germany, Institute of Nanotechnology, Karlsruhe Institute of Technology, 76344 Eggenstein-Leopoldshafen, Germany, Physikalisches Institut, Karlsruhe Institute of Technology, 76131 Karlsruhe, Germany, DFG-Center for Functional Nanostructures, Karlsruhe Institute of Technology, 76131 Karlsruhe, Germany, Institut de Physique et Chimie des Matériaux de Strasbourg (IPCMS), UMR 7504 CNRS-ULP, 67034 Strasbourg, France, Graduate School of Advanced Integration Science, Chiba University, Chiba 263-8522, Japan, and Institut für Theorie der Kondensierten Materie, Karlsruhe Institute of Technology, 76131 Karlsruhe, Germany

E-mail: Alexej.Bagrets@kit.edu

[*]To whom correspondence should be addressed
[†]Steinbuch Centre for Computing, Karlsruhe Institute of Technology, 76344 Eggenstein-Leopoldshafen, Germany
[‡]Institute of Nanotechnology, Karlsruhe Institute of Technology, 76344 Eggenstein-Leopoldshafen, Germany
[¶]Physikalisches Institut, Karlsruhe Institute of Technology, 76131 Karlsruhe, Germany
[§]DFG-Center for Functional Nanostructures, Karlsruhe Institute of Technology, 76131 Karlsruhe, Germany
[‖]Institut de Physique et Chimie des Matériaux de Strasbourg (IPCMS), UMR 7504 CNRS-ULP, 67034 Strasbourg, France
[⊥]Graduate School of Advanced Integration Science, Chiba University, Chiba 263-8522, Japan
[#]Institut für Theorie der Kondensierten Materie, Karlsruhe Institute of Technology, 76131 Karlsruhe, Germany
[@]Max-Planck-Institut für Festkörperforschung, 70569 Stuttgart, Germany

I. Atomic structure of H_2Pc on Mn/Fe(001)

A. Methodology

To identify an adsorption geometry of H_2Pc molecule on Mn/Fe(001) film, we have carried out electronic structure calculations based on density functional theory using a pseudopotential method as implemented in the SIESTA code.[1] A local spin density approximation (LSDA) to the exchange and correlation energy has been employed using the parametrization of Perdew and Zunger.[2] To further refine the calculation of the molecule-substrate interaction, the generalized gradient approximation[3] (GGA) was merged with the Grimme's correction scheme[4] to account for van der Waals interactions. Both systems, Mn/Fe(001) substrate and H_2Pc/Mn/Fe(001), were modeled using periodic supercell structure with each cell separated from its neighbors by a 15Å vacuum gap to ensure a minimal interaction between repeated images. The Brillouin-zone was meshed by a Monkhorst-Pack[5] grid with $4 \times 4 \times 1$ k-points. The standard Troullier-Martins[6] pseudopotentials are adopted and expressed in the Kleinman-Bylander[7] factorization. The double-ζ atomic orbitals have been used as the basis sets with an equivalent plane-wave cutoff of 500 Ry to represent the charge density.

B. Structural properties of Mn/Fe(001) films

First, we have examined the optimal growth of Mn layers on a Fe(001) surface. In fact, bulk Mn can be stable only in simple *bcc* or *fcc* crystal structures by alloying or epitaxial growth at room temperature.[8] Concerning the epitaxial growth, Mn layers grow on Fe(001) in the *bct* structure[9,10] with an in-plane lattice constant *a* equals to the interatomic distance of the substrate's surface layer.

In the present work, the Mn/Fe(001) substrate is modeled by 3 monolayers (ML) of Mn deposited on three layers of bcc Fe(001) (see Suppl. Fig. 1). A simulation cell contains 294 atoms, with 49 atoms in each layer. A calculated optimal distance between the Mn layers and the Fe(001) substrate is about 3 Å in the out-of-plane and 2.858 Å in the in-plane direction. This structure can be regarded rather as a body centered tetragonal *bct* with $c/a \sim 1.05$, which is in agreement with

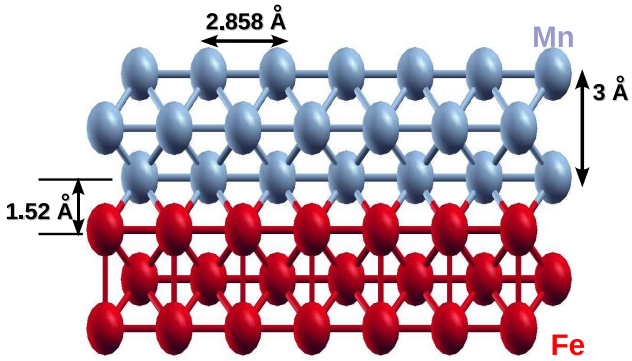

Suppl. Fig. 1: Three monolayers of Mn deposited on Fe(001).

that found by Krüger *et al.*[10]

In order to determine an adsorption geometry of the H_2Pc on Mn/Fe(001) substrates, we have checked four high-symmetry positions, i.e., the *center* and *top* positions where the H_2 atoms of the H_2Pc molecule are placed either in the center of the square or on top of Mn atom of the Mn/Fe(001) substrate, and the two equivalent *bridge* positions (see Suppl. Fig. 2).

C. Adsorption geometries of H_2Pc on Mn/Fe(001)

Concerning the stability of H_2Pc on Mn/Fe(001), we found that the *center* and the *top* positions (see Suppl. Fig. 3) are the most stable and the optimal distance between the molecule and the substrate is 2.1 Å within the LSDA. Computed relative energies of the optimized structures of H_2Pc adsorbed on Mn/Fe(001) are listed in Suppl. Table 1 for each of the adsorption sites. The total energy as a function of the distance between the molecule and the substrate is displayed in Suppl. Fig. 3. The figure shows that the difference between the total energy of *top* and *center* adsorption sites at 2.1 Å is small. Indeed, both curves are lower in energy compared to that of the *bridge* position. Switching to GGA and Grimme's correction scheme for vdW interactions[4] reduced further the molecule-surface distance to 1.93 Å but the *top* position remains the most favorable.

Suppl. Table 1: Calculated relative energy ΔE (eV), within the LSDA functional, for different adsorption geometries. The energy for the most stable position is set to zero.

	top	center	bridge
ΔE(eV)	0.0	0.06	3.1

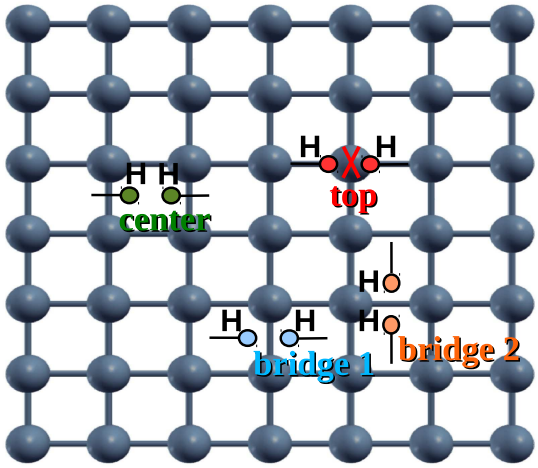

Suppl. Fig. 2: Adsorption geometry of H_2Pc on Mn/Fe(001) surface.

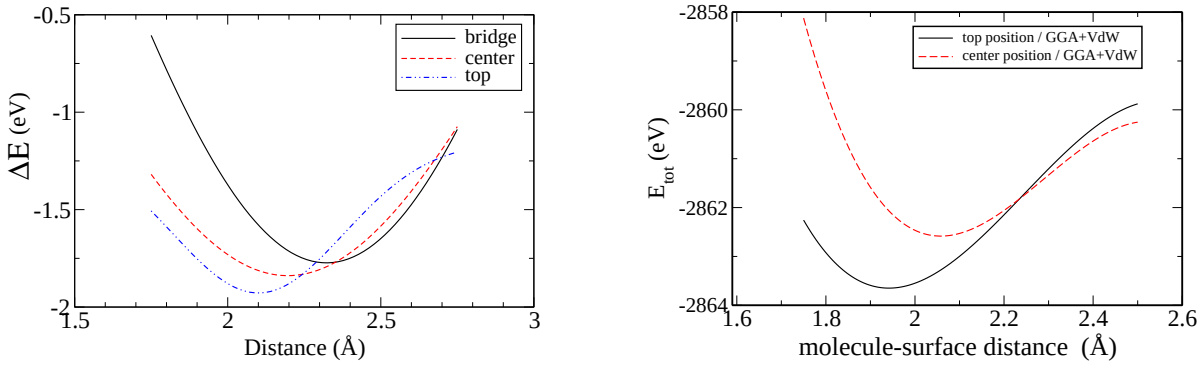

Suppl. Fig. 3: Energy *vs* the distance between H_2Pc and Mn/Fe(001) substrate for different adsorption geometries. The left panel represents the LSDA results and the right panel those within the GGA + vdW Grimme's correction scheme.

II. Binding of H_2Pc to the Fe STM tip

In this section we discuss a possible binding mechanism between the H_2Pc and the Fe coated STM-tip. As shown in Fig. 1 of the paper, STM tips are simulated by bcc (001) atomic clusters of Fe, containing either 14 atoms ("sharp" tip) or 13 atoms ("flat" tip). Since only one phenyl ring of the molecule is found in close proximity with the tip, it is essentially enough to consider binding of a benzene molecule to the Fe atomic cluster. We assume that such binding could be realized via the overlap between the highly directional *d* orbitals of the low-coordinated Fe atoms of the tip with the carbon p_z (out-of-plane) orbitals. In the case of "sharp" tip, we consider that Fe apex atom is bound to a single C atom (Suppl. Fig. 4a, inset). In the case of "flat" Fe tip, four out of six C atoms of the benzene ring are facing the corresponding Fe atoms of the cluster ensuring effective overlap between orbitals (inset of Suppl. Fig. 5a).

To estimate a binding distance *D* of the benzene ring to the Fe cluster(s), we have performed ground state energy calculations considering *D* as the only relevant parameter and keeping fixed all other interatomic distances. We have employed modern full-electron electronic structure code FHI-aims,[11] which is based on the numerical atom-centered basis sets. The PBE exchange correlation functional and the "tier1" basis set (of the split-valence plus polarization quality) have been used. Furthermore, van der Waals contribution to the ground state energy has been accounted for within the Tkatchenko-Scheffler model,[12] which relies on the interatomic dispersion coefficients derived from electron density.

Our results for the binding energy, $E_{\text{binding}} = E_{\text{mol}-\text{tip}} - E_{\text{mol}} - E_{\text{tip}}$, are shown in Suppl. Figs. 4 and 5. Indeed, we observe that a benzene molecule binds to the Fe clusters. In the case of "sharp" tip, a binding energy is around 0.75 eV at the optimal distance of 4.04 Å. Note that van der Waals forces contribute up to $\approx 50\%$ to the bond energy. In the case of "flat" tip, because of the larger number of C atoms involved, the binding energy is sufficiently larger, around 2 eV, allowing for the smaller molecule-to-tip distance of 3.78 Å. As follows from Supp. Fig. 5, this bond may be quantified as predominately covalent, since 70% of the binding energy is already given by the PBE functional, which does not account for the dispersion van der Waals interactions.

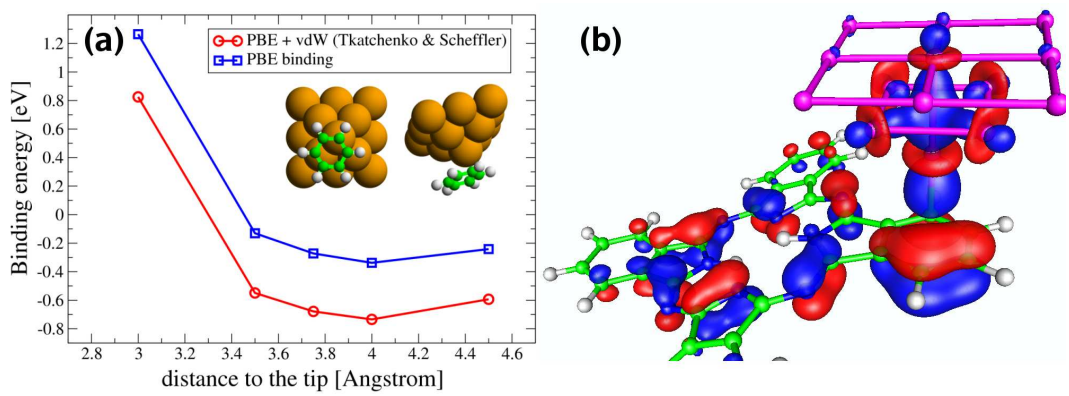

Suppl. Fig. 4: (a) Binding energy of the benzene molecule to the apex atom of the Fe cluster with 14 atoms (exact atomic geometry is given in the inset). Red and blue curves show, respectively, full binding energy (including dispersion vdW forces) and a contribution to the bond energy due to a covalent overlap between Fe and C orbitals. (b) A hybrid molecular orbital of the H_2Pc bound to the Fe cluster, which illustrates a directional covalent-like character of the bond.

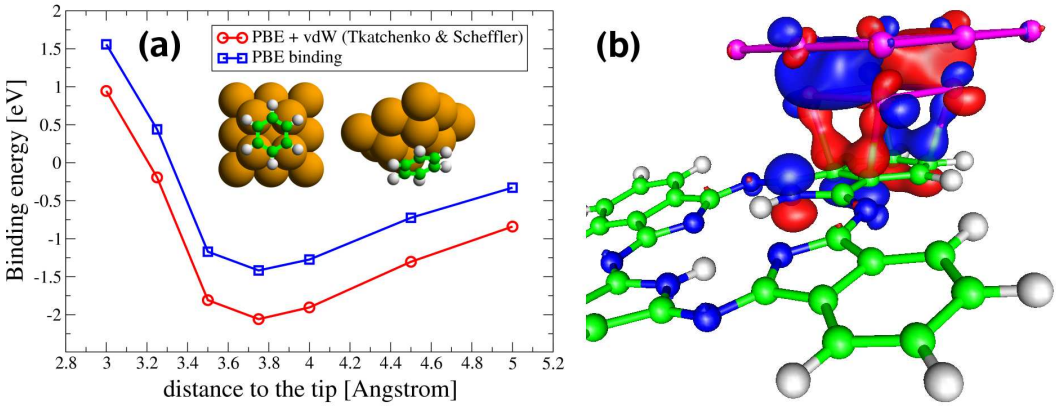

Suppl. Fig. 5: The same as in Supp. Fig. 4 but for the case of Fe cluster with 13 atoms.

To further support our statements, we present in Suppl. Figs. 4b and 5b selected hybrid wave functions of the H_2Pc bound to the Fe atomic clusters. Wave functions plots correspond to hybird states in the majority spin channel placed approx. 4 eV below the Fermi level. Both hybrid molecular orbitals show significant overlap between formely delocalized π orbitals of the phenyl ring with those Fe *d* like orbitals that point towards C atoms. Such a covalent-like hybridization distorts the perfect conjugation of the involved side phenyl ring of the H_2Pc.

III. Electronic structure of Fe(001)/H_2Pc/Mn/Fe(001) junctions

A. TURBOMOLE

Methodology

Density functional theory (DFT) based electronic structure and transport calculations through H_2Pc molecular junctions were performed within the non-equilibrium Green's function (NEGF) approach as implemented in a homemade simulation code[13] AITRANSS (abbrev. stands for *ab initio* transport simulations) interfaced to the quantum chemistry package TURBOMOLE.[14] An approach, which we follow here, is quite similar to that chosen in our previous work.[15] Two slightly different atomic configurations of the "extended molecule" used to simulate a bottle-neck of molecular junctions are shown in Figs. 1a and 1b (see text of the paper): H_2Pc is bound to the two bcc(001)-like clusters, with 13 (or 14) and 28 atoms, representing an Fe tip and a Mn surface, respectively. As argued in the previous section, in the case of a "flat" tip geometry (Fig. 1a), four Fe atoms are bound to four C atoms of the molecule's side group, while in the case of a "sharp" tip geometry (Fig. 1b), an Fe apex atom forms a bond to only one C atom. Furthermore, the geometry of H_2Pc molecule, initially placed at *top* position on the bcc Mn cluster, was later on fixed by bending along the low-energy vibrational eigenmode ($\omega = 15.5$ meV). This choice was motivated by earlier experiments, as discussed previously.[15,16] The GGA (BP86 functional[17]) and a contracted Gaussian-type split-valence basis set with polarization functions (SVP)[18] were used for calculations.

First, a closed-shell (nonmagnetic) solution was found for the "extended molecule" comprising either 1304 electrons (case of a "flat" Fe tip, Fig. 1a) or 1330 electrons (case of a "sharp" Fe tip, Fig. 1b). To account for infinite reservoirs with spin-polarized electrons, spin-dependent ($\sigma = \pm 1/2$) local self-energies, $\Sigma_\sigma^{\mathrm{sub/tip}}(\mathbf{x},\mathbf{x}') = \left[\lambda + \sigma\Delta_{\mathrm{ex}}^{\mathrm{sub/tip}} - i\gamma\right]\delta(\mathbf{x}-\mathbf{x}')$, were ascribed to the outermost boundaries of the simulation clusters. Here, a parameter $|\Delta_{\mathrm{ex}}^{\mathrm{sub/tip}}| = 1.43$ eV accounts for exchange splitting of the *d*-states of the Fe surface at the bottom of the *d* band.[19] (At this point we imply that a few atomic layers thick Mn film is deposited on the Fe substrate, which is an experimental situation.) A freedom to choose a sign of $\Delta_{\mathrm{ex}}^{\mathrm{sub/tip}}$ independently for the "substrate"

and "STM tip" clusters allowed us to achieve two solutions with a parallel (P) and antiparallel (AP) alignment of the magnetizations of the Fe tip and the Mn surface.

We have applied the NEGF to evaluate the charge- and spin-density matrices in the presence of open boundaries, respecting charge neutrality within the “extended molecule”. In an iterative scheme, the density matrices computed by AITRANSS module are returned to TURBOMOLE to find a modified set of Kohn-Sham orbitals, with a cycle to be repeated unless the self-consistent solution is reached. For a given value γ ($= 1.36$ eV in present calculations) of the level broadening, the contribution λ to the real part of the self-energy is defined by imposing the condition that the charge on the outermost surfaces of the simulation cluster approaches the bulk value. An initial guess for the charge- and spin-density matrices has been prepared in such a way that Mn spins within the "substrate" cluster reflect antiferromagnetic (AF) ordering of magnetizations between the surface- and next-to-the-surface atomic layers. We have insured that AF ordering is also preserved when self-consistency is reached.

Electronic structure of Fe tip and Mn substrate.

One can deduce from Suppl. Fig. 6 that within our approach a desired solution reflecting magnetic ordering within the Fe tip and the Mn surface is indeed achieved. Namely, the density of states at the Fe tip is spin-polarized (here we consider the case of a “sharp” STM tip, Fig. 1b of the paper), with the majority spin band being almost occupied and the minority spin band being centered around the Fermi level. Based on the Löwdin population analysis, we found out magnetic moments of $2.52\mu_B$ at the Fe apex atom of the tip and $2.87\mu_B$ at four next-to-the-apex atoms. These values are slightly larger that the bulk magnetic moment of bcc-Fe ($\approx 2.2\mu_B$) due to a lower coordination number. Electronic states at the Mn surface are even stronger spin-polarized with exchange splitting $\simeq 4$ eV being roughly twice as large as compared to Fe. According to our calculations, Mn surface atoms have (Löwdin) magnetic moments around $4.1\mu_B$. This implies that an electronic configuration of Mn is close to $3d^6 4s^1$ where one s electron (per atom) is redistributed among the two spin bands. Due to the AF ordering, negative (and smaller) magnetic moments, around $-3.0\mu_B$, have been found within the next-to-the-surface atomic plane of Mn.

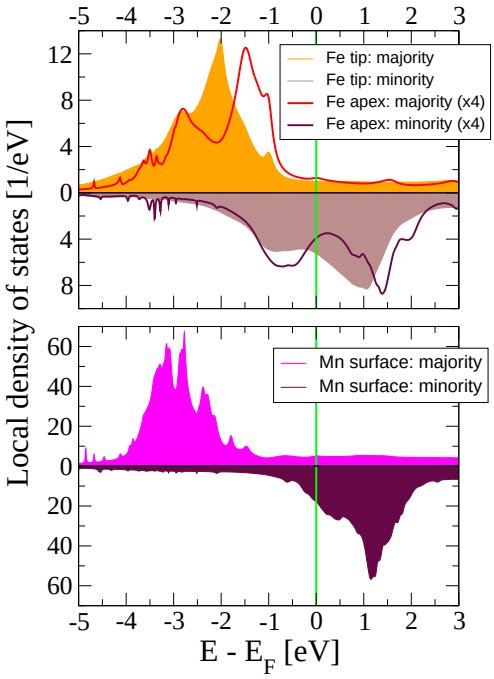

Suppl. Fig. 6: Local density of states at the Fe tip (apex and four neighboring atoms are distinguished) and at the Mn (001) surface atomic layer (sum over 16 atoms). The case of parallel alignment of spins in the Fe tip and the Mn surface is shown.

Spin-selective hybridization of electronic states at H_2Pc.

To provide further arguments in support of our discussion (cf. text of the paper) on the formation of spin-polarized states at H_2Pc and on-resonance LUMO transport, we present in Suppl. Figs. 7 and 8 the local density of states (LDoS) at H_2Pc and its projection on frontier molecular orbitals, a highest occupied molecular orbital (HOMO) and a lowest unoccupied molecular orbital (LUMO) doublet. We observe that LDoS at the vicinity of the Fermi level is dominated by LUMOs implying a charge transfer (around $1.2e$) from Mn surface to H_2Pc. In case of weak hybridization to the metal states, LUMO orbitals show up as sharp resonances. This is realized for the majority (α) channel in the case of a "flat" tip geometry and P alignment of Fe tip and Mn-surface magnetizations (Suppl. Fig. 7a), as well as for the majority (α) spins in the case of a "sharp" tip geometry, both for P and AP alignment of magnetizations (Suppl. Fig. 8a,c). In contrast, for the minority (β) channel, due to a substantial hybridization to the minority spin Mn states, LUMO orbitals exhibit much broader structures (quasi-bands) in the LDoS with long tails spreading above the Fermi level (see Suppl.

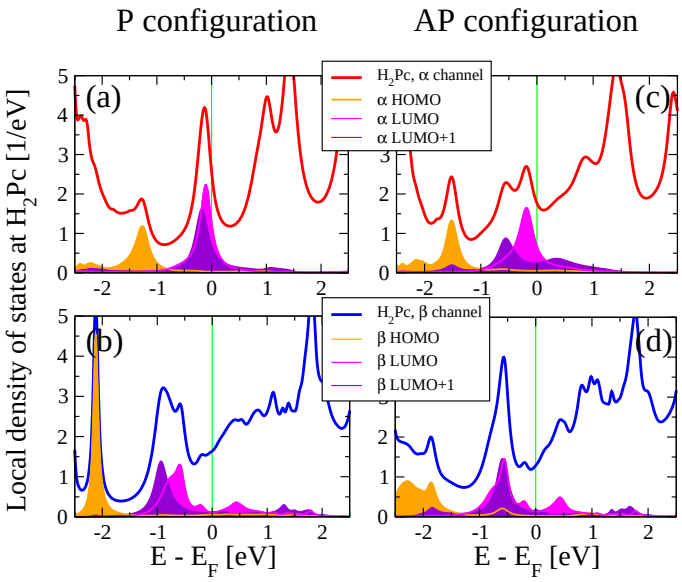

Suppl. Fig. 7: A case of the "flat" Fe tip: shown is the spin-dependent local density of states (LDoS) at H_2Pc molecule, and contributions to it due to HOMO (orange color) and a LUMO doublet (violet and magenta colors). Left column of plots refers to the parallel (P) alignment of magnetizations of the Fe tip and the Mn surface, right column refers to the antiparallel (AP) alignment.

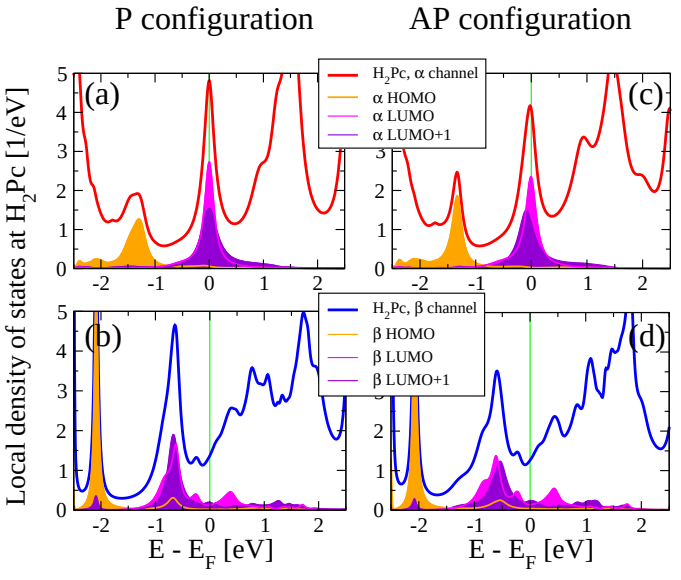

Suppl. Fig. 8: The same as in Suppl. Fig. 7 but for the case of H_2Pc molecule attached to a “sharp” Fe tip.

Figs. 7b,d and 8b,d). As we stressed in the text of the paper, peculiarities in the spin-dependent LDoS at H_2Pc molecule are transferred to the energy-dependent transmission function, which therefore acquires a dependence on spin and gives rise to a magnetoresistance effect. Finally, we mention that a significant charge transfer to the LUMO doublet (slightly larger than one electron per spin channel) is partially compensated by the leakage of charge from occupied molecular levels.

B. SIESTA/SMEAGOL

Method

We have also performed complementary studies of electronic structure of a H_2Pc/Mn/Fe(001) system employing SIESTA[1] and SMEAGOL[20] codes. These codes are based on a pseudopotential method and numerically localized pseudoatomic orbitals forming a basis set for the valence electrons. For the exchange and correlation potential, the LSDA was used as parametrized by Perdew and Zunger[2] for non-metallic and metallic systems. The standard Troullier-Martins[6] pseudopotentials were adopted and expressed in the Kleinman-Bylander[7] factorization. In our calculations, we used double-ζ atomic orbitals as the basis set with an equivalent plane-wave cutoff of 500 Ry to represent the charge density. For the structural optimizations, a conjugate gradient method was employed, with a force at each atom converged below 0.04 eV/Å.

Results

Before examining electronic properties of a H_2Pc molecule deposited on a Mn/Fe(001), we have checked electronic structure of the isolated H_2Pc. The resulting density of states (DoS) is shown in Suppl. Fig. 9 plotted *vs* the Fermi level, E_F, of the Mn/Fe(001) substrate. The H_2Pc molecule is characterized by energetically isolated HOMO and LUMO levels located at -0.55 eV and 0.87 eV below and above E_F, respectively, with the HOMO-LUMO gap about ~ 1.42 eV. We observe that the quasi-degenerate LUMO is projected both on C and N atoms, while the HOMO does not have a weight on nitrogens, in agreement with our previous calculations.[15]

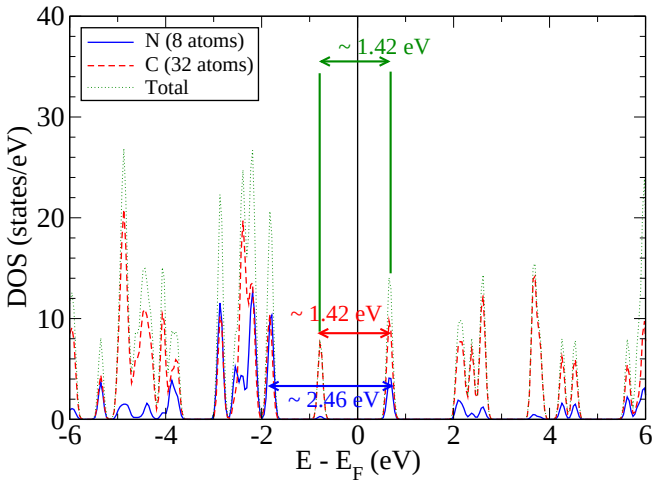

Suppl. Fig. 9: Density of states (DoS) of isolated H_2Pc plotted *vs* the Fermi level of Mn/Fe(001) substrate.

Further, on Suppl. Fig. 10, we compare DoS of the first and second Mn layer of the substrate alone and with that calculated when the H_2Pc is deposited at the *center* position on a Mn surface. The H_2Pc has negligible effect on Mn DoS, which clearly confirms an antifferomagnetic ordering between neighboring atomic planes. The observed exchange splitting is, however, larger than that found within a quantum chemistry based method (cf. Suppl. Fig. 6). This can be attributed to different exchange-correlation functionals (LSDA *vs* GGA) and basis sets used and points out to a known sensitivity in the prediction of a position of the localized *d* bands of transition metals on employed methodologies.

We now focus on the effect of Mn/Fe(001) substrate on the electronic structure of H_2Pc molecule. For that, we show in Suppl. Fig. 11 DoS projected at various atoms of H_2Pc, namely, the two central H atoms, and both N and C atoms which are nearest neighbors to the central H atoms. For the majority spin states (upper plot), we observe a gap of ~ 1.5 eV between HOMO and LUMO resonances, with the LUMO peak placed just above the Fermi level and the HOMO peak positioned ~ 1.2 eV below E_F. In the minority spin channel (lower plot), the LUMO orbital is much stronger hybridized with the substrate and develops a broader structure around E_F which spreads down to -1.0 eV. The HOMO resonance is shifted to approx. -2.0 eV. The picture resembles a close similarity to that shown on Suppl. Figs. 7 and 8, and implies a charge transfer from the H_2Pc on the Mn surface, in a full agreement with our previous discussion.

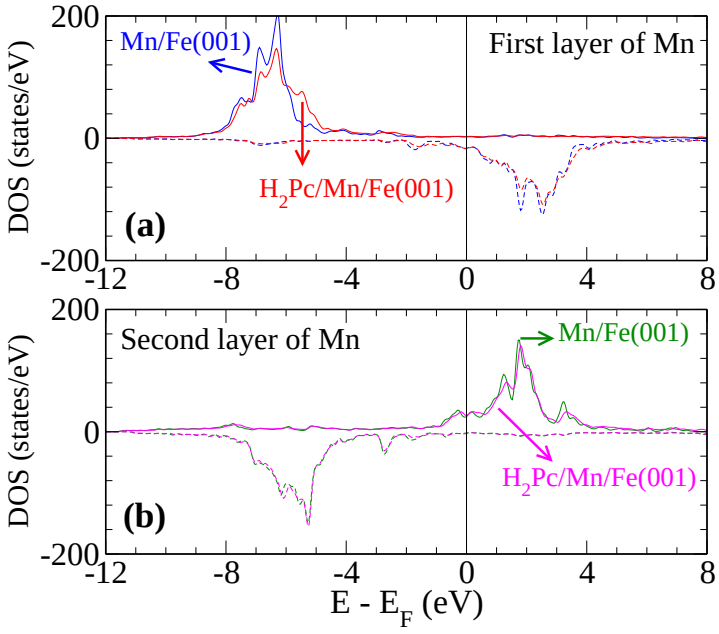

Suppl. Fig. 10: Density of states at the surface (a) and at the next-to-the-surface (b) atomic layers of a bcc Mn film for the two systems: Mn/Fe(001) and H_2Pc/Mn/Fe(001).

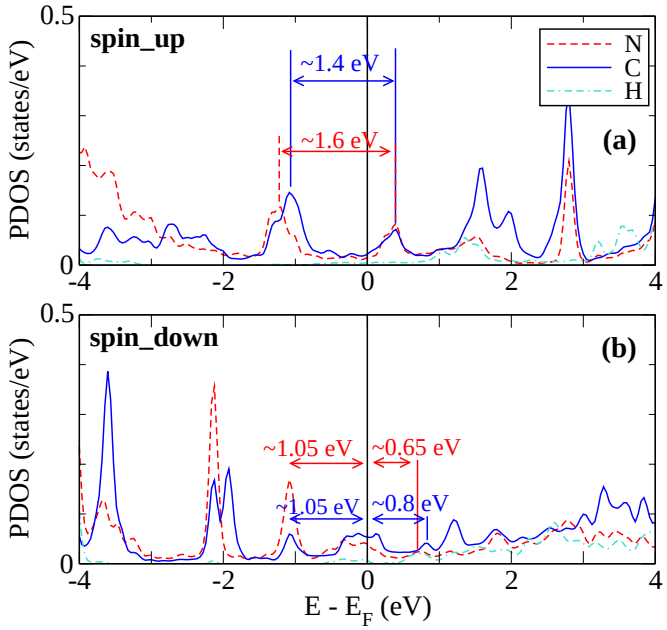

Suppl. Fig. 11: Partial density of states (PDoS) of H_2Pc deposited on Mn/Fe(001) projected on N and C atoms, which are nearest neighbors to the central H atoms of the molecule.

References

(1) J. M. Soler, E. Artacho, J. D. Gale, A. Garcia, J. Junquera, P. Ordejon, and D. Sánchez-Portal, J. Phys. Condens. Matter **14**, 2745 (2002). E. Artacho, D. Sánchez-Portal, P. Ordejón, A. García, and J. M. Soler, Phys. Stat. Sol. B **215**, 809 (1999); D. Sánchez-Portal, E. Artacho, and J. M. Soler, Int. J. Quantum Chem. **65**, 453 (1997); P. Ordejón, E. Artacho, and J. M. Soler, Phys. Rev. B **53**, R10441 (1996).

(2) J. P. Perdew and A. Zunger, Phys. Rev. B **23**, 5048 (1981).

(3) J. P. Perdew, K. Burke, and M. Ernzerhof, Phys. Rev. Lett. **77**, 3865 (1996).

(4) S. Grimme, J. Comput. Chem. C **27**, 1787 (2006).

(5) H. J. Monkhorst and J. D. Pack, Phys. Rev. B **13**, 5188 (1976).

(6) N. Troullier and J.-L. Martins, Phys. Rev. B **43**, 1993 (1991).

(7) L. Kleinmann and D. M. Bylander, Phys. Rev. B **48**, 1425 (1982).

(8) R. Pfandzelter, T. Igel, and H. Winter, Surf. Sci. **389**, 317 (1997).

(9) S. K. Kim, Y. Tian, M. Montesano, F. Jona, and P. M. Marcus, Phys. Rev. B **54**, 5081 (1996).

(10) P. Krüger, O. Elmouhssine, C. Demangeat, J. C. Parlebas, Phys. Rev. B **54** 6393 (1996).

(11) V. Blum, R. Gehrke, F. Hanke, P. Havu, V. Havu, X. Ren, K. Reuter, and M. Scheffler, Comp. Phys. Comm. **180**, 2175-2196 (2009).

(12) Alexandre Tkatchenko and Matthias Scheffler, *Phys. Rev. Lett.* **102**, 073005 (2009).

(13) A. Arnold, F. Weigend, and F. Evers, J. Chem. Phys. **126**, 174101 (2007).

(14) TURBOMOLE V5.10 by R. Ahlrichs *et al.* (www.turbomole.com)

(15) S. Schmaus, A. Bagrets, Y. Nahas, T. K. Yamada, A. Bork, M. Bowen, E. Beaurepaire, F. Evers, and W. Wulfhekel, Nature Nanotech. **6**, 185–189 (2011).

(16) A. F. Takács, F. Witt, S. Schmaus, T. Balashov, M. Bowen, E. Beaurepaire, and W. Wulfhekel, Phys. Rev. B **2008**, *78*, 233404.

(17) (a) A. D. Becke, Phys. Rev. A **38**, 3098 (1988); (b) J. P. Perdew, Phys. Rev. B **33**, 8822 (1986).

(18) A. Schäfer, H. Horn, and R. Ahlrichs, J. Chem. Phys. **97**, 2571 (1992).

(19) S. Ohnishi, A. J. Freeman, and W. Weinert, Phys. Rev. B, **28**, 6741–6748 (1983).

(20) A. R. Rocha, V. Garcia-Suárez, S. W. Bailey, C. J. Lambert, J. Ferrer, and S. Sanvito, Phys. Rev. B **73**, 085414 (2006)